Chapter 7

Functional Analysis of Novel Coiled-Coil Proteins in *Streptomyces coelicolor* and their Role in the Control of Growth and Morphogenesis

Katherine Celler, Joost Willemse and Gilles P. van Wezel

Manuscript in preparation.

ABSTRACT

In the morphologically complex streptomycetes, reproduction occurs via specialized aerial hyphae that produce chains of unigenomic spores, involving an unusually complex process of coordinated cell division and DNA segregation. Cytoskeletal elements play an important structural role in this process, and mutants of *Streptomyces coelicolor* lacking the cytoskeletal genes *filP*, *mreB* or *scy* show various defects in the integrity and shape of aerial hyphae and spores. Here we show that the tandem gene sets SCO2259-2260 and SCO3285-3286, which encode hitherto unstudied proteins containing coiled-coil motifs, play an important role in facilitating sporulation-specific cell division and morphogenesis. SCO2259 and SCO3285 localize in large evenly-spaced foci in young aerial hyphae, while SCO3286 forms long filaments inside immature spores. Scanning and transmission electron microscopy revealed aberrant and branching spore chains in SCO2259 and SCO3286 mutants, while SCO3285 mutants demonstrated chains with misaligned spores. Notably, null mutants lacking the flotillin-domain protein SCO3286 demonstrated enhanced frequency of spore chain formation, with many short and branching spore chains. Deletion of both SCO3286 and SCO3285 inhibited sporulation, with a small number of spores that were highly sensitive to heat treatment. Our results highlight the intricate role of cytoskeletal genes in the *Streptomyces* developmental program.

INTRODUCTION

For bacteria, maintaining the proper cell shape during growth and division is important for survival of progeny. Cytoskeletal elements play an important role in coordinating these processes, with actin-homologs MreB and Mbl working to maintain shape during growth of rod-shaped bacteria (Jones *et al.* 2001; Carballido-Lopez and Errington 2003; Kruse, *et al.* 2005), and tubulin-homolog FtsZ forming the scaffold for the contractile ring (the Z-ring) during cell fission (Bi and Lutkenhaus 1991). In addition, an abundance of coiled-coil rich proteins exists in other bacteria to enable a great diversity of cellular architectures - such as spiral (Specht *et al.* 2011), crescent (Ausmees *et al.* 2003), or filamentous (Bagchi *et al.* 2008). For a detailed account of the bacterial cytoskeleton, the reader is referred to Chapter 2 of this thesis.

Perhaps due to their complex morphogenesis and multicellular lifestyle, the streptomycetes are particularly rich in cytoskeletal and coiled-coil proteins proposed to be cytoskeletal in nature (Letek *et al*. 2012). In addition to MreB and Mbl (Mazza *et al.* 2006; Heichlinger *et al.* 2011), and FtsZ (McCormick *et al.* 1994; Schwedock *et al.* 1997), sequence analysis has identified more than ten putative coiled-coil cytoskeletal proteins encoded for in streptomycete genomes, most of which have yet to be characterized (Table 1).

Table 1. *Confirmed and putative cytoskeletal proteins in Streptomyces.*

Protein	Annotation[1]	Reference
SCO2082, FtsZ	Cell division protein; homolog of tubulin	(McCormick *et al.* 1994; Schwedock *et al.* 1997)
SCO2611, MreB	Rod-shape determining protein; homolog of actin	(Mazza *et al.* 2006)
SCO2451, Mbl	Rod-shape determining protein; homolog of actin	(Heichlinger *et al.* 2011)
SCO1407	Hypothetical protein	
SCO2259, ScyB	Multi-domain regulatory protein	
SCO2260, ScyC	Putative membrane protein	
SCO3285, ScyD	Large glycine/alanine-rich protein	
SCO3286, ScyE	Putative secreted protein	
SCO3542	Putative transferase	
SCO5396, FilP	Filament-forming protein	(Bagchi *et al.* 2008)
SCO5397, Scy	*Streptomyces* cytoskeletal element	(Walshaw *et al.* 2010; Holmes *et al*. 2013

[1] Annotations adapted from StrepDB, the Streptomyces Annotation Server (http://strepdb.streptomyces.org.uk/).

Proteins rich in coiled-coil motifs are capable of self-assembly into filaments *in vitro*, forming flexible filaments which are resistant to strain and have strong mechanical properties, necessary to maintain cell integrity (Herrmann and Aebi 2004).

Unlike rod-shaped bacteria, which grow by lateral cell-wall extension, *Streptomyces* hyphae grow apically, with new material deposited at hyphal tips. Critical for control of apical growth is coiled-coil protein DivIVA (Flärdh 2003; Flärdh 2010). DivIVA is a homolog of MinE, and in *Bacillus subtilis* controls the localization of the cell division inhibitors MinCD, contributing to septum positioning (Edwards and Errington 1997). That DivIVA orchestrates cell-wall synthesis in the streptomycetes suggests that its role has changed during evolution, along with the different mode of growth (Claessen *et al.*, *submitted*). Its depletion or overproduction results in aberrant branching and altered hyphal characteristics. In *M. tuberculosis*, interaction between DivIVA and penicillin-binding protein PBP3, supports the role of DivIVA as a polarity marker that recruits the cell-wall machinery during polarized growth (Mukherjee *et al.* 2009). Recent results show that DivIVA is part of a larger tip-organizing center in the streptomycetes, colocalizing with several other proteins and complexes. These include, among others, the coiled-coil rich cytoskeletal proteins FilP (Bagchi *et al.* 2008) and Scy (Walshaw *et al.* 2010), as well as the cell-wall remodeling protein SsgA (Noens *et al.* 2005).

Rich in coiled-coil domains, FilP is important for the stability of the hyphae and for correct DNA segregation (Bagchi *et al.* 2008; Fuchino *et al.* 2013). Atomic force microscopy (AFM) demonstrated that *filP*-deletion mutants have weaker hyphae than the wild-type strain. In vitro, FilP forms a cis-interconnected network, demonstrating the mechanistic basis for its control of rigidity (Fuchino *et al.* 2013). Encoded by a gene immediately upstream of *filP*, Streptomyces cytoskeletal protein Scy was recently proposed to control polarized growth in existing hyphal tips, as well as to promote new tip formation during branching (Holmes *et al.* 2013). Deletion of *scy* affects polarized growth and as a consequence also hyphal geometry, resulting in irregular hyphal width, short hyphal length and aberrant branching.

The cytoskeletal machinery also plays an important role in control of cell division. In most bacteria, the precise localization of the division septum at mid-cell involves the action of negative control systems such as the Min system, which prevents Z-ring assembly at the cell poles (Raskin and de Boer 1997; Marston *et al.* 1998) and nucleoid occlusion that prevents the formation of the Z-ring over non-segregated chromosomes (Wu and Errington 2004). FtsZ is the first to localize to the future division site, and subsequently initiates the recruitments of the other divisome proteins to construct the cell division Z-ring. Cell division in the streptomycetes occurs via a completely different mechanism, perhaps explained by

the lack of a mid-cell reference point in the multinucleoid hyphae. During growth of the vegetative mycelium, crosswalls form at irregular intervals to separate the syncytial cells into compartments. For more details on the mechanism of crosswall formation, the reader is referred to Chapter 4. Nutrient depletion then triggers the formation of the reproductive aerial myelium. During sporulation-specific cell division, FtsZ first forms long filaments in aerial hyphae, followed by focal points, and then ladders (Schwedock *et al.* 1997; Grantcharova *et al.* 2005; Willemse and van Wezel 2009). Eventually, following a complex process of coordinated cell division and DNA segregation (McCormick 2009; Jakimowicz and van Wezel 2012), cytokinesis results in the formation of long chains of unicellular spores.

Aerial septation in *Streptomyces coelicolor* was the first demonstrated case of positively-controlled cell division, with FtsZ recruited by the membrane-associated divisome component SsgB, and SsgB in turn recruited by SsgA (Willemse *et al.* 2011). SsgA and SsgB are members of the SsgA-like protein family (SALPs), which occur exclusively in the morphologically complex actinomycetes (Traag and van Wezel 2008). Ensuring the viability and integrity of these spores is critical for survival of progeny and it is little wonder that the cytoskeleton plays an important role in this respect. In fact, actin homologs MreB and Mbl, which support rod-shaped growth in *E. coli* and *B. subtilis* are essential for the integrity of the spore wall in *Streptomyces*. In addition, other members of the family of SsgA-like proteins (SsgC-G) function to control the build-up of septal peptidoglycan during sporulation and finally also its autolytic degradation during spore maturation (Noens *et al.* 2005).

Here we characterize two sets of novel cytoskeleton-related proteins in S. coelicolor, which we have termed Streptomyces cytoskeletal element ScyB (SCO2259) and ScyC (SCO2260) as well as ScyD (SCO3285) and ScyE (SCO3286), demonstrating their role in sporulation specific cell division.

RESULTS

As a first step towards the characterization of the genes with proposed, but as yet unknown, cytoskeletal functions (Table 1), cosmid-insertion mutants were obtained, and SsgA-, SsgB- and FtsZ-eGFP localization analyzed in the mutants. A basic analysis of membranes and cell wall, as well as live-dead staining analysis was performed using stains FM5-95, wheat germ agglutinate (WGA) and propidium iodide (PI) with SYTO 82, respectively. FM5-95 is an analog of FM4-64, which labels the plasma membrane, preferentially associating with membranes enriches in negatively charged phospholipids such as phosphatidylglycerol (PG) and cardiolipin (CL) (Sun and Margolin 1998; Pogliano *et al.* 1999; Grantcharova *et al*. 2003);

and WGA labels N-acetylglucosamine and N-acetylneuraminic acid (sialic acid) residues, which are found in newly-forming cell wall (Wright 1984; Schwedock *et al.* 1997). PI and SYTO 82 are routinely used in live-dead staining experiments (Fernandez and Sanchez 2001); PI is a non-cell-permeating nucleid acid stain which therefore stains dead cells and SYTO 82 is a green fluorescent stain which labels nucleic acids in all cells - both those with damaged and non-damaged membranes. Based on these initial experiments, we decided to focus on genes SCO2259, SCO2260 and SCO3285 and additionally SCO3286, which is co-transcribed with SCO3285, for further analysis; these mutants demonstrated promising phenotypes with increased FtsZ-ladder formation.

Using COILS, a program which identifies coiled-coils in protein sequences (Lupas, *et al.* 1991), the location and abundance of the coiled-coil motifs in the selected genes were determined (Figure 1). Domains predicted with more than 50% certainty are shown, and their size denoted by the bar length indicated.

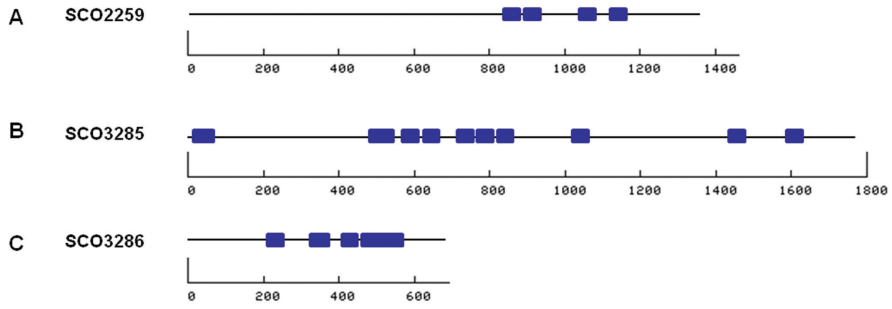

Figure 1. *Predicted coiled-coil domains in ScyB (SCO2259), ScyD (SCO3285) and ScyE (SCO3286). Location and size of motifs predicted with more than 50% certainty are indicated, based on output from the COILS Server from the ExPASy Bioinformatics Resource Portal (Lupas et al. 1991). ScyC (SCO2260) does not contain coiled-coil motifs.*

SCO2259 encodes for a large protein with one certain and several predicted coiled-coil domains. SCO2260 does not contain coiled-coil domains, but is potentially a site-2 protease (S2P) class of metalloproteases (MEROPS family M50) which cleaves transmembrane domains of substrate proteins, regulating intramembrane proteolysis of diverse signal transduction mechanisms. It may therefore have an influence on cellular differentiation and lipid metabolism, as prokaryotic S2P/M50 homologs have been shown to regulate stress responses, sporulation, cell division and differentiation (Marchler-Bauer *et al.* 2013). In *E. coli*, the S2P homolog RseP is involved in the sigmaE pathway of extracytoplasmic stress responses (Akiyama *et al*. 2004), and in *B. subtilis*, the S2P homolog SpoIVFB is involved

in the pro-σ^K pathway of spore formation (Lu *et al*. 1995). SCO3285 and SCO3286 show perfect co-occurrence, strongly suggesting a functional relationship, though they do not occur in all streptomycetes. The proteins encoded for by these genes are rich in coiled-coil domains. SCO3285 codes for a very large protein (>1700 amino acids in length), with a conserved ATPase domain which is putatively involved in DNA repair, while SCO3286 codes for a flottilin-domain protein. The genes have highly similar orthologues in *Pseudomonas* and other distant microbes.

Considering the coiled-coil domains of SCO2259, SCO3285 and SCO3286 and the role of the proteins in morphogenesis (see below), we tentatively designated them ScyB (SCO2259), ScyC (SCO2260), ScyD (SCO3285) and ScyE (SCO3286).

Transcriptional analysis by promoter probing

To roughly localize the promoters of the genes and assess their strength *in vivo*, we used the *redD* promoter-probe system (van Wezel *et al.* 2000c). For this purpose, DNA fragments containing the upstream region of all genes were cloned into promoter-probe vector pIJ2587, so as to place it in front of the promoterless *redD* gene. The resulting constructs were introduced in *S. coelicolor* A3(2) M512 (Floriano and Bibb 1996), which lacks the pathway-specific transcriptional activator genes *redD* and *actII-ORF4* for the biosynthesis of the pigmented antibiotics undecylprodigiosin and actinorhodin, respectively. Cloning of a DNA fragment with promoter activity in pIJ2587 allows transcription of *redD*, resulting in production of the red-pigmented and nondiffusible undecylprodigiosin (Red), which can easily be assessed visually or spectrophotometrically. Transformants were grown on R2YE plates supplemented with thiostrepton for 5 days. Production of the red-pigmented undecylprodigiosin (Red) was strongly stimulated by the *scyE* promoter and weakly by the *scyB* and *scyD* promoters (Figure 2). This indicates that all genes have their own promoter, although on the basis of gene organization we cannot rule out that *scyD* may be transcribed at least in part from P_{scyE}.

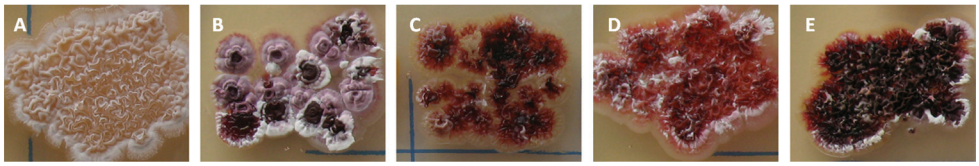

Figure 2. *Initial localization of promoters in the scyB, scyC, scyD and scyE upstream regions by promoter probing. S. coelicolor M512 harbouring (A) empty vector pIJ2587; (B) pGWS1111 (scyB upstream region); (C) pGWS1112 (scyC upstream region); (D) pGWS1113 (scyD upstream region); and (E) pGWS1114 (scyE upstream region). All upstream regions stimulated transcription of redD, as visualized by the red-pigmented patches of the respective transformants. Plates were grown on R2YE plates with thiostrepton as selective marker.*

Construction of in-frame deletion mutants

To construct in-frame deletion mutants, we replaced the entire coding region of each gene of interest by the apramycin cassette (*aacC4*) flanked by *loxP* sequences. For each experiment five transformants exhibiting the desired double-crossover phenotype ($Apra^R$ $Thio^S$) were selected and verified by PCR as described in the *Materials and Methods*. Following removal of the *aacC4* cassette by the Cre recombinase, deletion mutants were obtained for *scyB* (M145 ΔSCO2259), *scyD* (M145 ΔSCO3285) and *scyE* (M145 ΔSCO3286). In addition, the *scyDE* double mutant was constructed. Considering that the genes located downstream of gene pairs are divergently transcribed, polar effects due to insertional gene replacements were not anticipated.

Despite many attempts, we were unable to obtain an IFD double recombinant of SCO2260. A cryo-scanning electron microscopy (cryo-SEM) analysis of the cosmid insertion mutant did not reveal appreciable differences from the wild-type phenotype and the results described in this chapter therefore do not include this mutant. Further study is necessary to properly characterize this gene.

Characterization of the mutants

Mutants were plated on an SFM agar plates for 5 days at 30 ºC with the parental strain M145. The *scyD* null mutant had a lighter grey appearance than the parent, *scyB* and *scyE* mutants showed darker grey pigmentation, while the *scyDE* double mutant had a white appearance. The observed enhanced and reduced pigmentation likely indicates disturbance in the production of the grey-pigmented spores. The mutants did not show appreciable differences in development when grown on minimal medium agar plates supplemented with mannitol or on R2YE agar plates (not shown).

Fluorescence microscopy (FM) analysis revealed that, though similar in phenotype to wild-type, *scyB* and *scyE* null mutants produced branching spore chains and some aberrant spores (Figure 3A-E). Most spore chains of the *scyD* mutant had spores which were not completely aligned within chains, and spore chains occasionally branched. The most obvious phenotypic change, however, was observed in the *scyDE* double mutant, which sporulated far less abundantly than the parental strain M145. The few spore chains that were found had large spores (up to three to four times the length of wild-type spores) within spore chains of regular-sized spores. Box-plot statistical analysis indicated that, on average, spores of the *scyB*, *scyD* and *scyE* null mutants had a length similar to that of wild-type spores, with average lengths of 0.78 ± 0.07 µm, 0.85 ± 0.07 µm and 0.74 ± 0.12 µm, respectively, compared to a wild-type average length of 0.85 ± 0.11 µm, while the *scyDE*

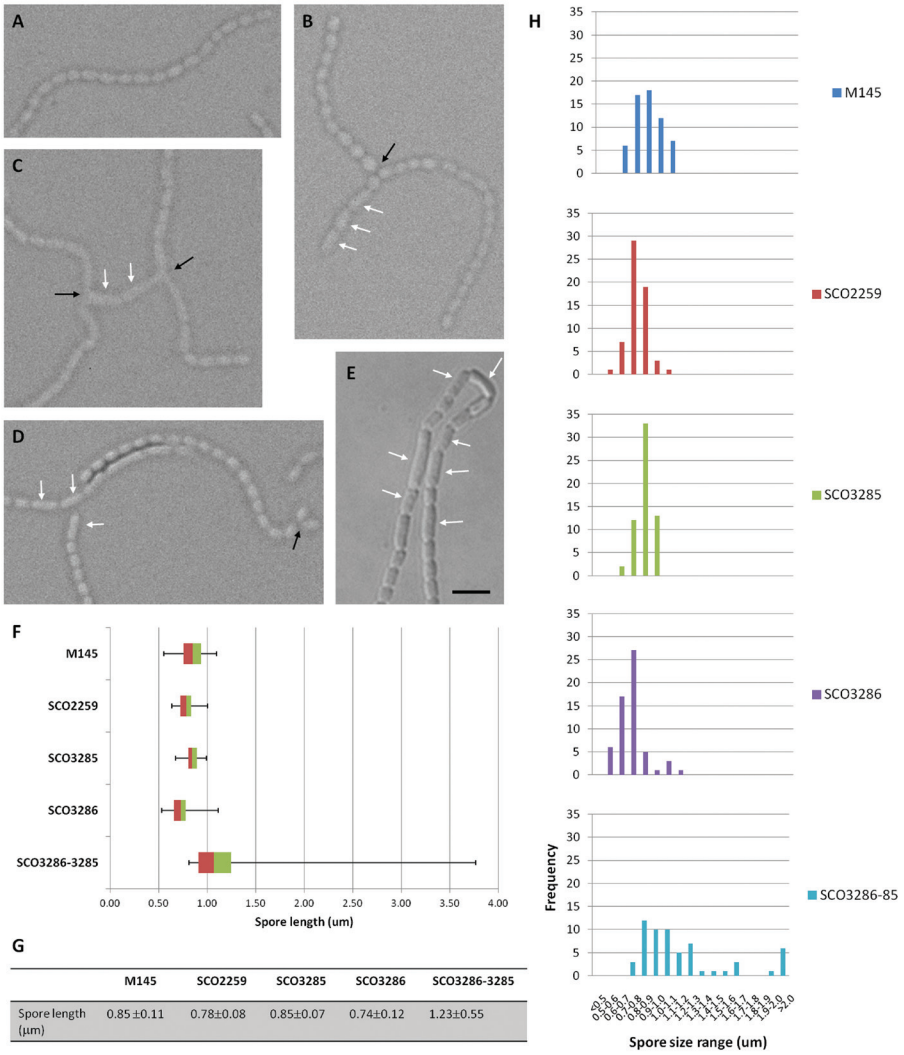

G

	M145	SCO2259	SCO3285	SCO3286	SCO3286-3285
Spore length (µm)	0.85±0.11	0.78±0.08	0.85±0.07	0.74±0.12	1.23±0.55

Figure 3. *Variation in spore size and chain length between mutants and wild type. Phase contrast micrographs of S. coelicolor M145 (parent; A) and its scyB (B), scyD (C), scyE (D) and scyDE null mutants. White arrows indicate aberrant spores in the deletion mutants, which appear to be delayed in formation and sometimes two or multiple times the size of wild type spores. Black arrows indicate branching spore chains. (F) Box plot of the spore length distribution in chains spores. Average spore length is given in (G). Spores of mutants scyB and scyE were on average slightly shorter, while spores of the scyDE double mutant were on average longer, sometimes up to two or three times the length of wild-type spores. Values are based on 60 spores measured by phase contrast microscopy. (H) Distributions of the spore lengths. Note that the size distribution of the scyDE double mutant is much broader than for the other strains. Scale bar, 2 µm, all images.*

double mutant had significantly larger spores, with greater variation, namely 1.23 ± 0.55 µm (Figure 3F). Distributions of the measurements indicate that the single mutants have narrow distributions, similar to that of the wild-type, while the double mutant *scyDE* has a very wide distribution, and irregular spore sizes. The large spores within the spore chains skew the distribution towards on average larger spore sizes than found in the wild-type strain.

Staining with FM5-95, WGA and DAPI was used to determine if the cell membrane, cell wall and DNA localization, respectively, was affected in the mutants (Figure 4). In particular, the *scyD* null mutant appeared different, with some membrane and wall material found at the external edges of forming spores. In the *scyDE* mutant, membrane and cell-wall staining within forming spore chains revealed that not all septa were at the same stage of completion. Staining with DAPI did not reveal significant differences in DNA segregation and condensation between mutants and the parental strain.

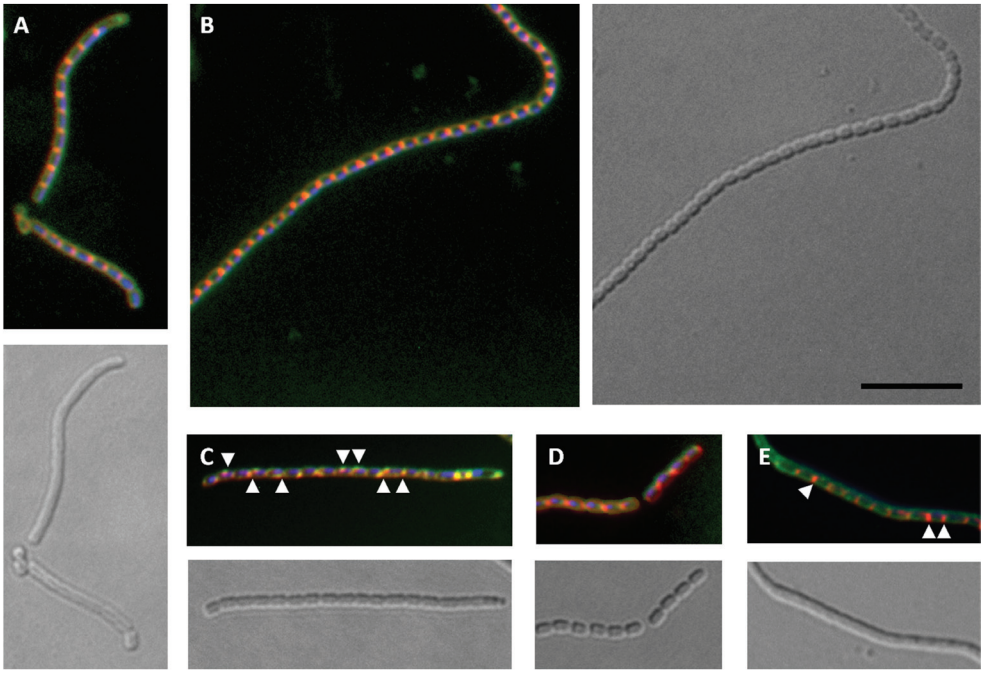

Figure 4. *Membrane (FM5-95; red), cell wall (WGA; green) and DNA (DAPI; blue) staining of sporogenic aerial hyphae of S. coelicolor M145 (parent; A) and its scyB (B), scyD (C), scyE (D) and scyDE mutants. Overlays of the three channels are shown, as well as a light image. The scyB mutant appeared similar to wild type. In scyD null mutants, some membrane and cell wall mislocalization was seen, with some staining of the edges of the spore exterior (arrows). The scyDE mutant showed enhanced membrane staining between spores within a chain (arrows), suggesting that spore maturation was at different stages of completion in those chains. Scale bar, 5 µm.*

Cryo-SEM revealed that *scyB* and *scyD* mutants develop similarly to the wild-type strain, although some spores were slightly irregular and not perfectly aligned within spore chains (Figure 5). The *scyE* null mutant was strongly affected in sporulation, however, with a multitude of short spore chains. Non-sporulating aerial hyphae were scarce, though all samples were grown for the same amount of time. In the *scyDE* double mutant spore chains were scarce. Those which were found appeared irregular, containing small and large spores.

Transmission electron microscopy (TEM) provided further detail of spore morphology (Figure 6). The *scyB* null mutant appeared most similar to wild-type, though branching spore chains were occasionally encountered (Figure 6B). The spore wall of the *scyD* null mutant appeared lighter than that of the wild type or of the other mutants (Figure 6C), but examining other micrographs indicated that this may be an artifact of fixation. TEM of the *scyE* mutant revealed that spores are slightly shorter and rounder (Figure 6D). The *scyDE* mutant occasionally produced larger spores, though most spore chains were regular (Figure 6E).

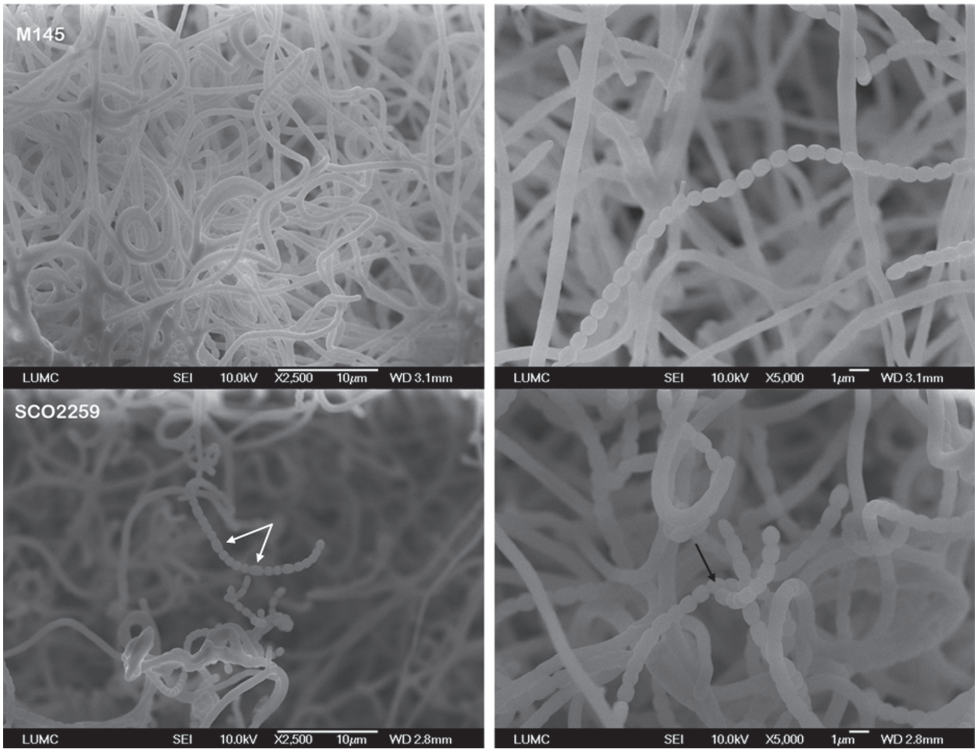

(Figure 5. continued on overleaf)

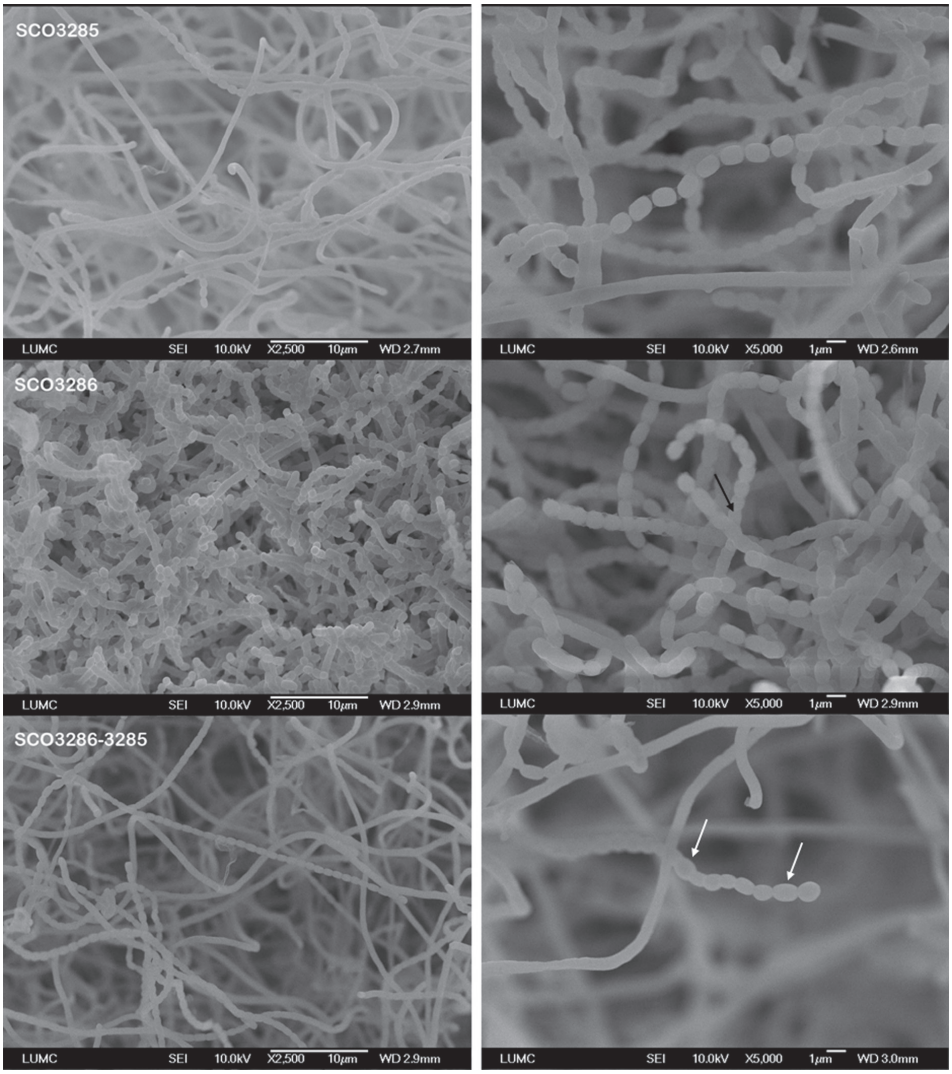

Figure 5. *Cryo-scanning electron micrographs of the scyB, scyD and scyE mutants and scyDE double mutant. The scyB mutant produced spores with up to twice the length of wild-type spores (white arrows), and branching spore chains (black arrow). The scyE mutant formed short spore chains, with certain spores appearing to branch (black arrow). The scyDE double mutant had few irregular spore chains (white arrows).*

Figure 6. *(Right) Transmission electron micrographs of the wild-type strain (A) and its scyB (B), scyD (C), scyE (D) and scyDE (E) null mutants. Black arrows indicate where spore chains appear to branch. The spore wall of the scyD null mutant was more electron-lucent than that of other samples, which is likely an artifact of fixation . Similar staining was seen in previous experiments for the wild-type strain. Spores of the scyE deletion mutant appear shorter and rounder than those of the wild type or the other mutants, while in the scyDE double mutant both longer (left) and normal (right) were found. Scale bar, 1 µm.*

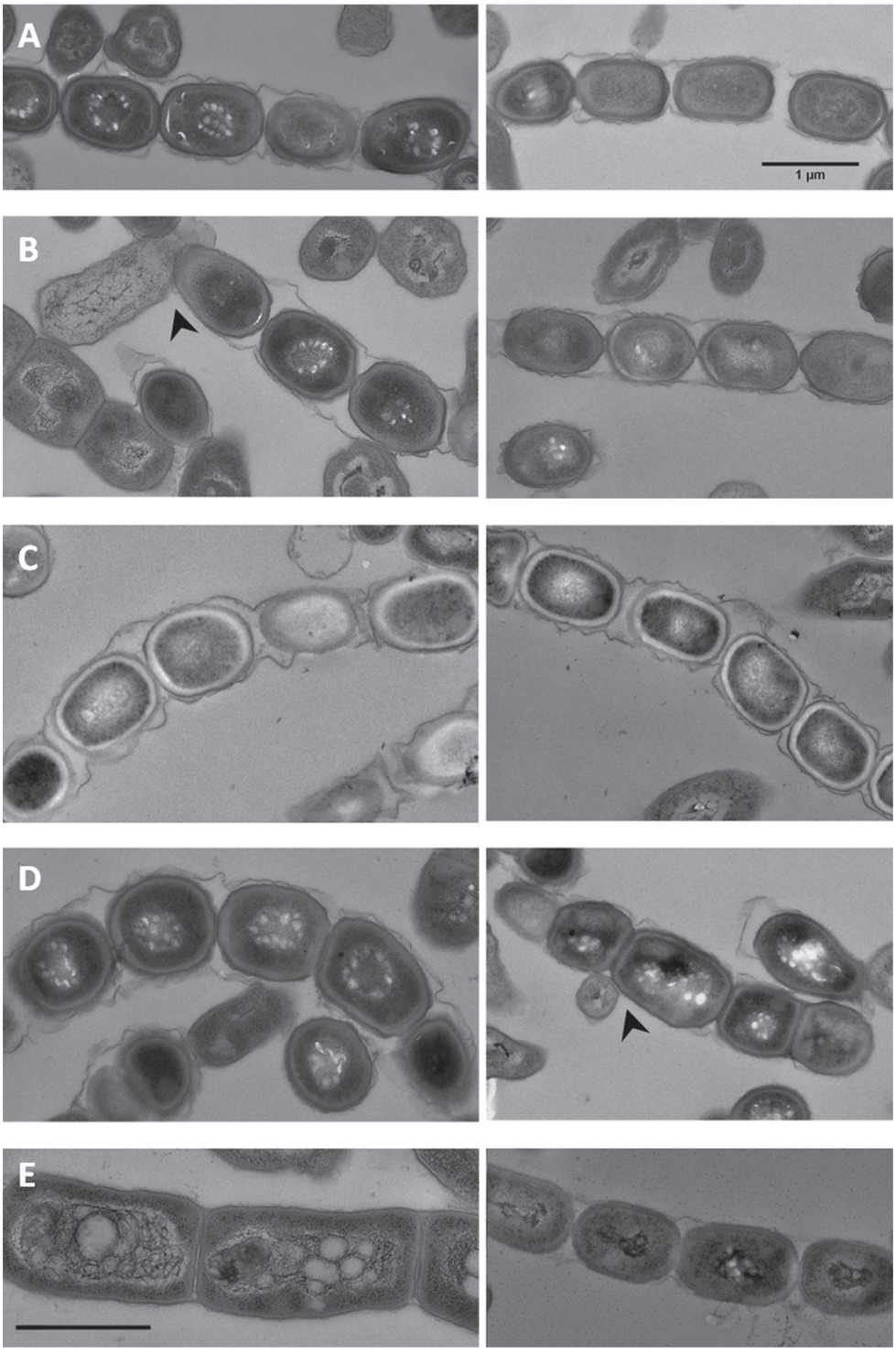
A
1 µm
B
C
D
E

To further investigate the effect of these mutations on sporulation and spore integrity, spore viability was determined by live-dead staining using PI and SYTO, and spores were tested for resistance to heat treatment and SDS buffer (see *Materials and Methods*). Wild-type spores are resistant to exposure at moderately high temperature as well as to treatment with SDS, which has, in fact, been reported to activate germination (Grund and Ensign 1982). In contrast, spores with compromised integrity show decreased survival rates upon heat and detergent treatment (Mazza *et al.* 2006; Willemse *et al.* 2012). Spores of the *scyB*, *scyD* and *scyE* null mutants were as viable in terms of colony forming units as those of the parental strain, but demonstrated decreased heat resistance (Figure 7). Treatment with SDS activated germination of these mutants, as in the wild-type (not shown). Only 75% of the untreated spores of the *scyDE* double mutant were viable, however, and these were very sensitive to heat and SDS. While 99% of wild-type spores were viable, and roughly 98% and 66% survived 10 or 20 minutes, respectively, of heat treatment, 10 minutes of heat treatment at 60 ºC was sufficient to kill all spores of the *scyDE* double mutant. Only roughly 60% of *scyDE* double mutant spores survived one hour of incubation at room temperature in 5% SDS.

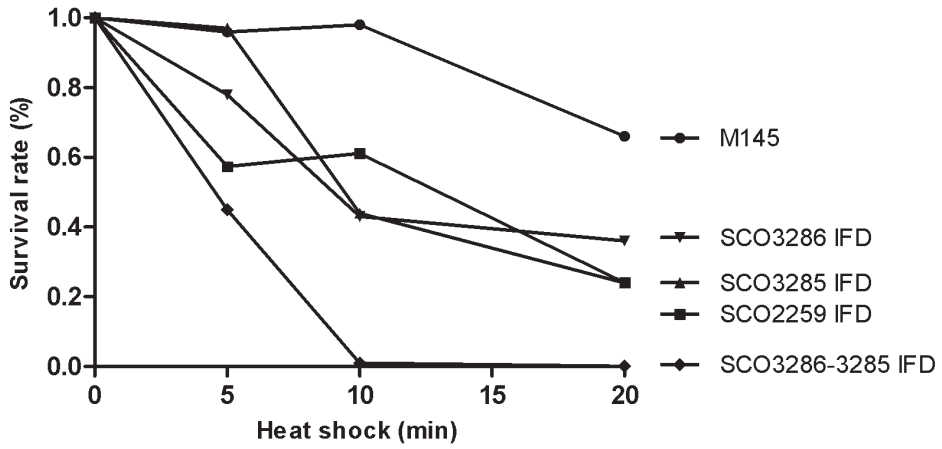

Figure 7. *Spore survival rate upon heat shock at 60 °C. The single deletion mutants show reduced resistance to treatment, compared to the wild-type, demonstrating affected spore integrity. In particular, the SCO3286-3285 (scyDE) double mutant was greatly affected, and no colony forming units remained after 10 minutes of heat treatment. IFD, in-frame deletion mutant.*

Protein localization and genetic complementation of mutants

To investigate the localization of the proteins, low copy-number vectors were constructed that harbor the respective genes and their upstream region followed by the gene for eGFP, so as to express C-terminal eGFP fusions from the natural promoters. In this way, plasmids pGWS1105 (for ScyB-eGFP), pGWS1106 (for ScyD-eGFP) and PGWS1107 (for ScyE-eGFP) were created, and introduced in the respective null mutants, as well as in the parental strain M145. Fluorescence microscopy indicated that ScyB-eGFP localized in large, sometimes somewhat oblong focal points along early aerial hyphae (Figure 8). With a similar pattern, ScyD-eGFP localized in large foci regularly positioned along aerial hyphae, appearing before the start of sporulation. ScyE-eGFP localized predominantly to the cell wall of aerial hyphae, at a somewhat later stage than ScyD, appearing before the completion of spore constriction. Portions of hyphae in which localization was observed demonstrated complete envelopment by filament-like structures. In an attempt to analyze the localization of ScyD and ScyE simultaneously, similar fusions as for eGFP were created using the red-fluorescent mCherry, but in this case the fluorescence of the chimeric proteins was too weak and the studies therefore not feasible.

The *scyB* and *scyE* null mutants could be fully restored to wild-type sporulation by the respective chimeric proteins, as shown by cryo-SEM (Figure 9). A light grey phenotype of the *scyD* null mutant containing pGWS1106 on plate (not shown) indicated a potential reduction of WhiE spore pigment; cryo-SEM, however, indicated the presence of spore chains similar to those of the wild-type (Figure 9). To see if complementation could be achieved with copies of the wild-type genes, constructs pGWS1108, pGWS1109 and pGWS1110 were created, which contain wild-type *scyB*, *scyD*, and *scyE* and upstream regions, respectively. Work is underway to assess if these constructs restore wild-type growth and development to the mutants.

Localization of FtsZ-eGFP in the mutants

Vector pFK41 (Grantcharova *et al.* 2005), which is an integrative vector that expresses FtsZ-eGFP from the *ftsZ* promoter region, was used to assess FtsZ localization in the mutants (Figure 10). While the parental strains showed typical spectacular Z-rings, aberrant Z-rings were observed in the mutants. In aerial hyphae of *scyB* and *scyE* mutants, ladders were evenly spaced, but not all were at the same stage of formation. Sometimes FtsZ localized partially at one side of a hyphae (red arrows in Figure 10), corresponding to the aberrant spore chains seen in SEM and TEM, in which not all spores within a chain were at the same stage of completion. In all mutants, upon spore formation, FtsZ localized to the spore wall

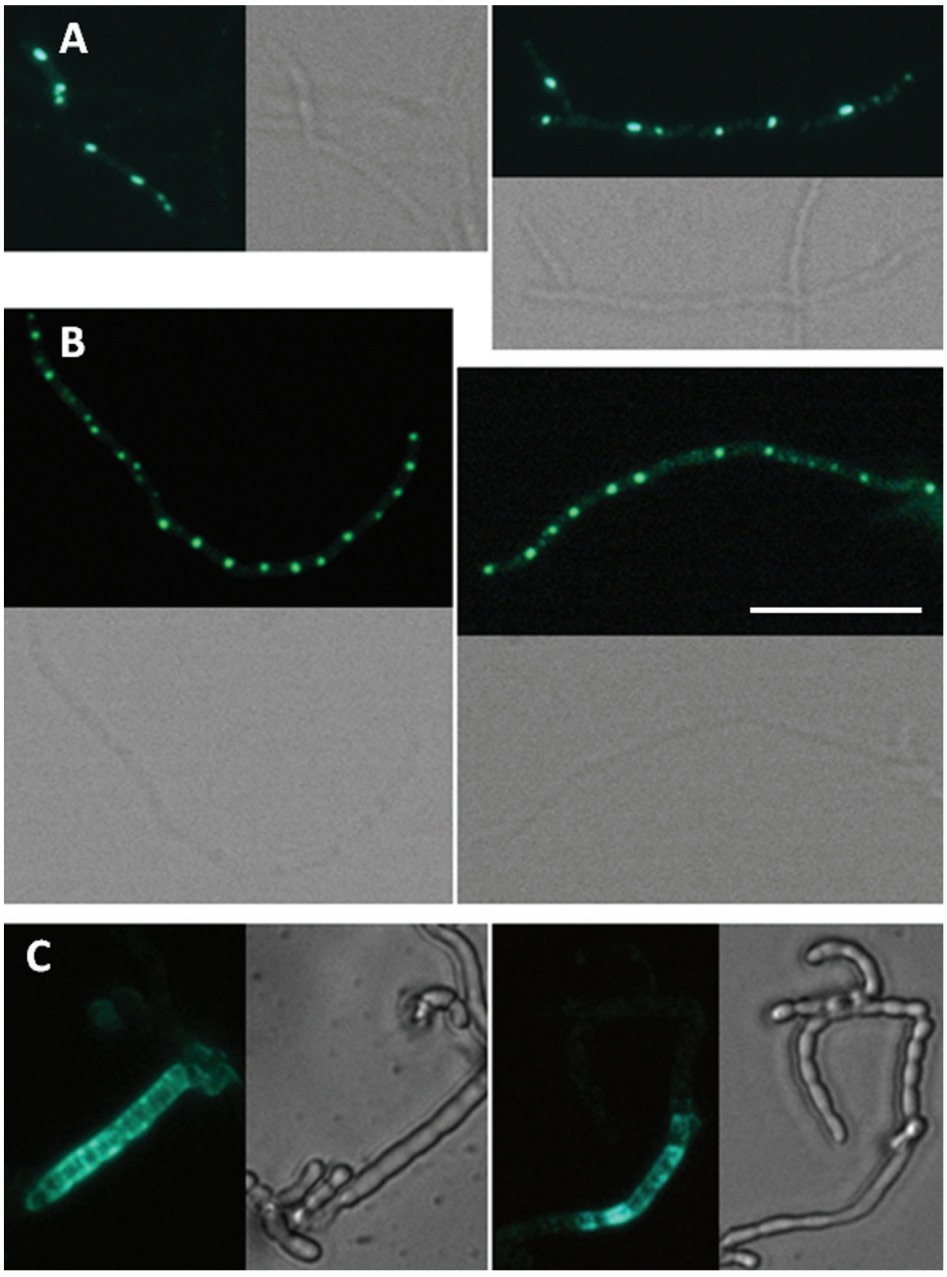

Figure 8. *Localization of ScyB and ScyD and ScyE. (A) In the scyB null mutant harboring pGWS1105, ScyB-eGFP localized in large (often oblong) foci in young aerial hyphae. (B) In the scyD null mutant harboring pGWS1106, ScyD-eGFP formed large foci at roughly 1 µm intervals. (C) In the scyE null mutant harboring pGWS1107, ScyE-eGFP formed filaments, which apparently enveloped the spores. Scale bar, 5 um, all images.*

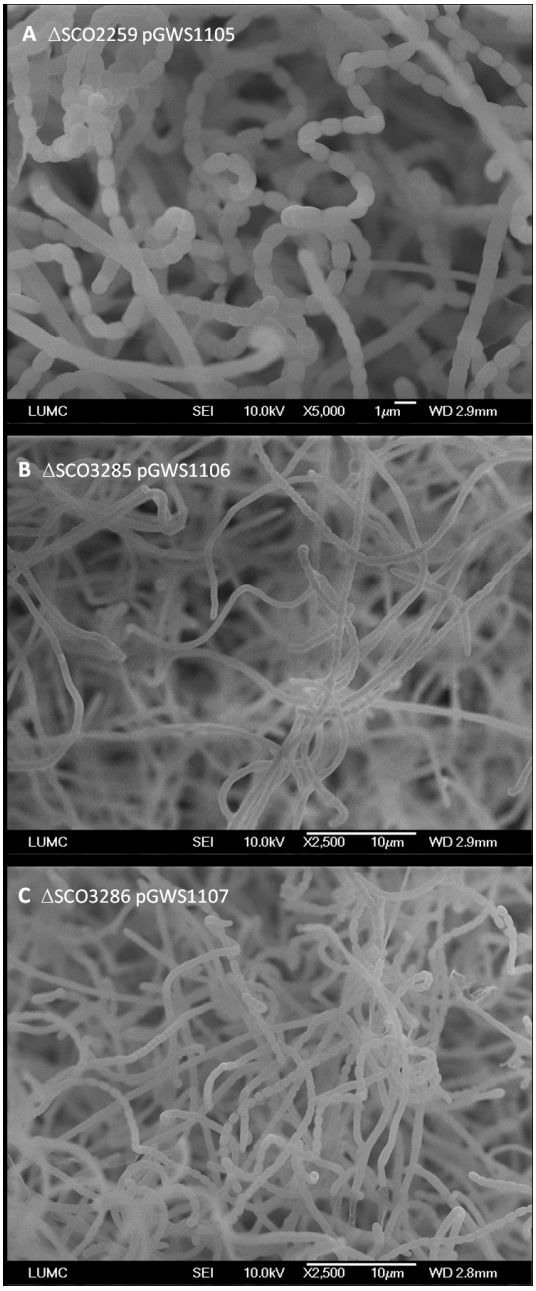

Figure 8. *Cryo-scanning electron micrographs of scyB (SCO2259) (A), scyD (SCO3285) (B), and scyE (SCO3286) (C) deletion mutants complemented with pGWS1105 (expressing ScyB-eGFP), pGWS1106 (expressing ScyD-eGFP) and pGWS1107 (expressing ScyE-eGFP), respectively. Mutants could be restored to wild-type sporulation by the respective chimeric proteins.*

(white arrows in Figure 10), which is not seen in wild type. In the *scyDE* double mutants, FtsZ localized diffusely, or formed filaments around aerial hyphae. Sometimes FtsZ ladders were seen, but these were irregular, seemingly occurring by change of the filamentous localization into more condensed localization. Again, when spores were formed, FtsZ localized to the spore wall.

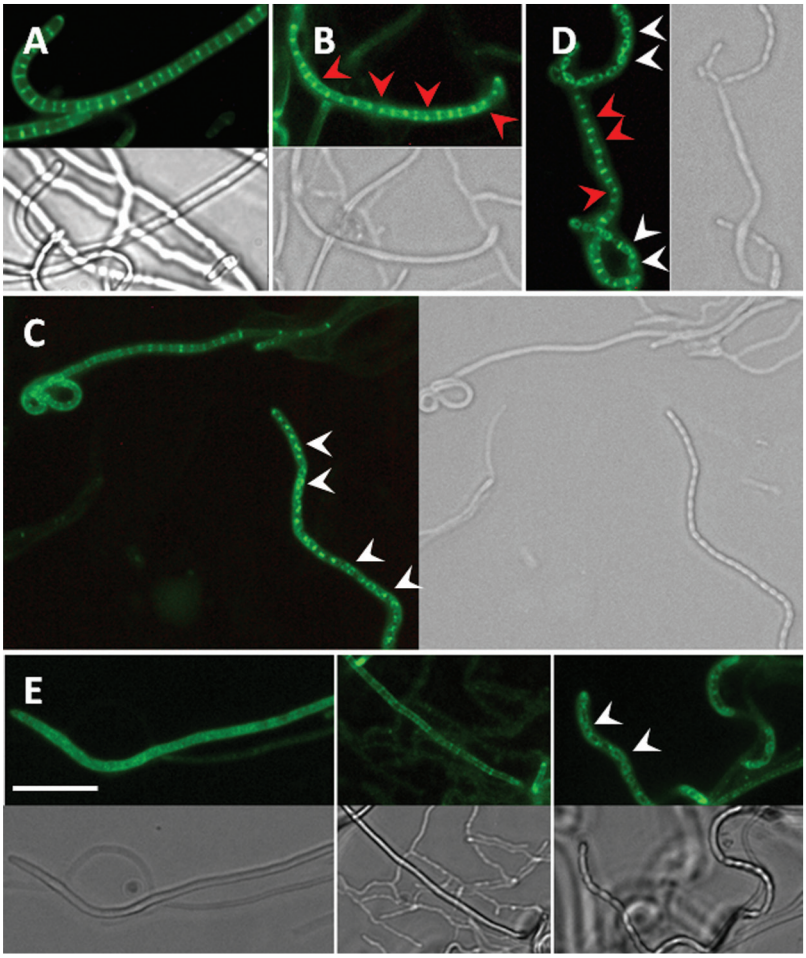

Figure 10. *Localization of FtsZ in the mutants. FtsZ-eGFP localization in (A) M145 pKF41, and its scyB (B), scyD (C), scyE (D) and scyDE null mutants. For the latter, three panels are presented showing FtsZ localization in young (left), pre-sporulation (middle) and sporulating (right) aerial hyphae. Partially formed FtsZ ladders indicated with red arrows; FtsZ localization to the spore wall indicated with white arrows. Scale bar, 5 µm, all images.*

DISCUSSION

Multiple cell division during sporulation of streptomycetes requires the coordination of septum-site localization and cell division with DNA replication and segregation (Flärdh and Buttner 2009; Jakimowicz and van Wezel 2012). This complicated process involves synchronized chromosome segregation and condensation by ParA and ParB (Ruban-Ośmiałowska, *et al.* 2006), as well as activation of sporulation-specific cell division by SsgA and SsgB (Willemse *et al.* 2011). In addition, the *whi* genes, so called because of the lack of pigmentation of the mutant colonies (Chater 1972), ensure the correct timing of developmental FtsZ production (Willemse *et al*. 2012). Ultimately, the process of division culminates in the formation of spectacular FtsZ-ladders and subsequently the division of aerial hyphae into unigenomic spores. Yet even if all the above morphological checkpoints are correctly passed, if spore integrity cannot be ensured, neither can the survival of progeny. Multiple cytoskeletal elements play a role at this point of the lifecyle, working to ensure that spores are resistant to desiccation and mechanical stress, able to lie dormant for years before germinating again in favorable conditions.

Structural support in cells is often provided by proteins with coiled-coil motifs, which are capable of self-assembly into filaments *in vitro*, forming a strong, yet flexible, mechanical basis for maintaining cell integrity. It is perhaps little wonder, given the complexity of the *Streptomyces* development program, that streptomycete genomes encode for numerous coiled-coil proteins, most with as yet unknown function. Those characterized (DivIVA, FilP and Scy) function during hyphal growth, ensuring strength of extending apical tips and forming part of a larger tip-organizing complex in *Streptomyces* (Flärdh 2010; Fuchino *et al.* 2013; Holmes *et al.* 2013). During development, several other cytoskeletal elements come in to play. Actin-homologs MreB and Mbl, which in rod-shaped bacteria are essential to maintain shape during growth, are not essential for vegetative growth in *Streptomyces coelicolor*, but rather for spore integrity (Mazza *et al.* 2006; Heichlinger *et al.* 2011), while the SsgA-like proteins SsgC-G are essential for the build-up and degradation of septal peptidoglycan (Noens *et al.* 2005). Mutations in these genes result in aberrant spore formation.

Here we show that coiled-coil rich proteins ScyB, ScyD and ScyE play an important role during spore formation in *Streptomyces* reproductive cell division. Deletion of *scyB* resulted in minor defects in sporulation; some uneven spore chain formation, and occasional large or branching spores. Containing one, and possibly more (up to four) coiled-coil domains, it is likely that this protein provides structural support during sporulation, while perhaps carrying out additional functions with its N-terminal domain. Deletion of *scyD* affected

deposition of new cell-wall material during sporulation. New wall material did not localize evenly to spore ends, and as a result, spore chains of *scyD* null mutants did not align correctly (end-to-end) within spore chains, but rather formed zig-zagging chains. Nevertheless, chromosome segregation and septation occurred synchronously, and spore viability was not compromised in the mutant. A major phenotypic difference was seen upon deletion of *scyE*, which encodes a flotillin homolog; null mutants showed dramatically enhanced sporulation, seen most clearly in TEM micrographs, and the creation of multiple spore chains of small, round spores. Flotillins are a divergent membrane protein family associated with lipid rafts in eukaryotes and characterized by the SPFH (Stomatin, Prohibitin, Flotillin and HflK/C) domain of unknown function and extended heptad repeat regions (Hinderhofer *et al*. 2009). A study on dynamin and flotillin homologues in *B. subtilis* demonstrated that dynamin orthologue DynA plays a role in cell division, colocalizing with FtsZ and affecting Z-ring formation, while flotillin seems to generate a local environment favoring membrane curvature and perhaps help to recruit cell division proteins to the division site (Dempwolff *et al.* 2012). Interestingly, almost perfect co-occurrence could be seen between ScyE and another flottilin-domain protein in *Streptomyces*, SCO3607 (STRING, database of known and predicted protein interactions, www.string-db.org). When SCO3607 was disturbed in *Streptomyces albus*, enhanced sporulation was observed (our unpublished results), suggesting that flotillin lipid-raft markers perhaps create regions where division is preferred, preventing its occurrence elsewhere. Absence of these domains results in accelerated spore maturation, abundance of cell division events and over-sporulation.

Interestingly, the simultaneous deletion of *scyDE* resulted in a white phenotype, explained by a dramatic decrease in cell division. It is therefore likely that these genes work in concert to enable the onset of reproductive cell division. In their absence, division still occurs, but much less frequently, and spores are often two, three or even four times the length of wild-type spores - though then with the requisite number or chromosomes, indicating that chromosome replication and segregation is not disturbed.

Localization of ScyB, ScyD and ScyE was performed using a low copy-number vector harboring each gene and its upstream region followed by the gene for eGFP, so as to express C-terminal eGFP fusions from the natural promoters. ScyB-eGFP localized in localized in large, sometimes somewhat oblong focal points along early aerial hyphae. With a similar pattern, ScyD-eGFP localized in bright fluorescent foci at roughly 1 µm intervals in early aerial hyphae, while the ScyE-eGFP fluorescent fusion localized to forming spore chains, enveloping them in filament-like structures.

Attempts at colocalization of proteins using mCherry fusions were not successful, due

to the low fluorescence. Work is underway to localize the combination of genes behind the strong *scyE* promoter and with an mCherry fusion at the C-terminus. Other technologies include immunoelectron microscopy for localization studies, and FRET-FLIM for in vivo colocalization and interaction studies. This should aid us in gaining further insight into the function and localization of the proteins and their interaction partners.

Summarizing, our work demonstrates that the coiled-coil proteins ScyB, ScyD and ScyE play a role in controlling morphogenesis, and in particular ensure correct sporulation-specific cell division. At this stage, it is yet unclear how they exert their functions. Considering that the proteins contain hallmarks of cytoskeletal proteins, such as the presence of coiled-coil domains and the effect of gene disruption on the integrity of the hyphae, we anticipate that they play a cytostructural role during the later stages of development. It is important to note that ScyD and ScyE are widespread in bacteria, including many that do not sporulate (such as Pseudomonas), strongly suggesting that they have a conserved function in the bacterial cell cycle that likely extends beyond the control of sporulation. Further studies should shed more light on whether indeed they form IF-like cytostructural elements, what their interactions partners are and how precisely they contribute to the control of morphogenesis in *Streptomyces*.

MATERIALS AND METHODS

Bacterial strains and media

The bacterial strains described in this work are listed in Table 2. *E. coli* K-12 strains JM109 (Sambrook *et al.* 1989) and ET12567 (MacNeil *et al.* 1992) were used for plasmid propagation, and were grown and transformed by standard procedures (Sambrook *et al.* 1989). *Streptomyces coelicolor* A3(2) was the parent for all mutant strains described in this work. All media and routine *Streptomyces* techniques are described in the *Streptomyces* manual (Kieser *et al.* 2000). Soy Flour Mannitol (SFM) medium was used for making spore suspensions and R2YE agar plates for regenerating protoplasts and, after the addition of appropriate antibiotic, for selecting recombinants. Phenotypic characterization of mutants was done on SFM, R2YE and on minimal medium agar plates with mannitol (MMman) as the sole carbon source (Kieser *et al.* 2000). For fluorescence microscopy, samples from liquid cultures were spotted onto a glass microscope slide before microscopy analysis. Images of vegetative hyphae from solid growth samples were collected from samples that had been inoculated at the acute-angle junction of coverslips inserted at a 30° angle in SFM agar plates.

Table 2. *Bacterial strains used in this study.*

Bacterial Strain	Genotype	Reference
S. coelicolor A3(2), M145	SCP1$^-$ SCP2$^-$	(Kieser *et al.* 2000)
S. coelicolor M512	M145 Δ*redD*Δ*actII-ORF4*	(Floriano *et al.* 1996)
	M145 SCO2259::*Tn5062, Apr*^{R}	This work.
	M145 SCO2260::*Tn5062, Apr*^{R}	This work.
	M145 SCO3285::*Tn5062, Apr*^{R}	This work.
	M145 ΔSCO2259	This work.
	M145 ΔSCO3285	This work.
	M145 ΔSCO3286	This work.
	M145 ΔSCO3286-3285	This work.
E. coli JM109	See reference.	(Sambrook *et al.* 1989)
E. coli ET12567	See reference.	(MacNeil *et al.* 1992)

Plasmids, constructs and oligonucleotides

All plasmids and constructs are summarized in Table 3. The shuttle vectors pHJL401 (Larson and Hershberger 1986) and pSET152 (Bierman *et al.* 1992) were used for cloning in *Streptomyces*, which both have the pUC ori for high-copy number replication in *E. coli* and the SCP2* ori on pHJL401 (around five copies per chromosome) and the *attp* sequence, allowing

integration at the attachment site of bacteriophage φC31, on pSET152 for maintenance in *S. coelicolor*. PCRs were done with Pfu polymerase (Stratagene), in the presence of 10% (v/v) DMSO. The oligonucleotides are listed in Table S1.

Insertion mutants were made using the Tn5062 transposon single-gene insertion knock-out cosmids (Fernandez-Martinez *et al.* 2011). For insertional inactivation of genes, transposon single-gene insert knock-out cosmids were used. For this, *E. coli* ET12567 containing puZ8002 was used for conjugation-mediated introduction of the relevant cosmids into pre-germinated spores of *S. coelicolor* M145. SCO2259 was removed by replacement with a recombinant cosmid harboring transposant 1G2.2.A05, SCO2260 by 1G2.2.C08, and SCO3285 by E39.2.C08.

The strategy for creating in-frame knock-out mutants is based on the unstable multi-copy vector pWHM3 (Vara *et al.* 1989). For each knock-out construct, roughly 1.5 kb of up- and downstream region of the respective genes were amplified by PCR from *S. coelicolor* genomic DNA and inserted into the instable multi-copy shuttle vector pWHM3 as described (van Wezel *et al.* 2005). For the exact location of the oligonucleotides, see Table S1. Fragments were inserted into pWHM3, and the engineered XbaI site was used for insertion of the apramycin resistance cassette *aacC4* flanked by *loxP* sites between the upstream and downstream flanking regions. The presence of the *loxP* recognition sites allows the efficient removal of the apramycin resistance cassette following the introduction of a plasmid pUWLcre expressing the Cre recombinase. We constructed the knock-out plamids pGWS1101, pGWS1102 and pGWS1103 for the single gene replacement of SCO2259, SCO3285 and SCO3286, respectively. Plasmid pGWS1104 was used for the double replacement of SCO3286-3285. To analyze correctness of the mutants, PCRs were done on mycelium from liquid-grown cultures, with oligonucleotide pairs as given in Table S1.

Table 3. *Plasmids and constructs*

Plasmid	Description	Reference
pHJL401	*Streptomyces/E.coli* shuttle vector (5-10 and roughly 100 copies per genome, respectively)	(Larson and Hershberger 1986)
pSET152	*Streptomyces/E. coli* shuttle vector (integrative in *Streptomyces*, high copy number in *E. coli*)	(Bierman *et al*. 1992)
pWHM3	Cloning vector, *colE1* replicos, psG4 replicon, Tsr^R, Amp^R	(Vara *et al*. 1989)
pUWLcre	pUWLoriT derivative with *cre(a)* gene under *ermE** promoter	(Fedoryshyn *et al.* 2008)
pIJ2587	Promoter probe vector containing promoterless *redD* gene	(van Wezel *et al.* 2000c)
pKF41	pSET152-derived integrative vector expressing FtsZ-eGFP	(Grantcharova *et al.* 2005)
pGWS1101	pWHM3 containing flanking regions of *S. coelicolor* SCO2259 with *apraloxP_*	This work.
pGWS1102	pWHM3 containing flanking regions of *S. coelicolor* SCO3285 with *apraloxP_*	This work.
pGWS1103	pWHM3 containing flanking regions of *S. coelicolor* SCO3286 with *apraloxP_*	This work.
pGWS1104	pWHM3 containing left-flanking regions of *S. coelicolor* SCO3286 and right-flanking regions of with *S. coelicolor* SCO3285 *apraloxP_*	This work.
pGWS1105	pHJL401 harboring SCO2259 behind its own promoter and fused to eGFP	This work.
pGWS1106	pHJL401 harboring SCO3285 behind its own promoter and fused to eGFP	This work.
pGWS1107	pHJL401 harboring SCO3286 behind its own promoter and fused to eGFP	This work.
pGWS1108	pHJL401 harboring SCO2259 behind its own promoter	This work.
pGWS1109	pHJL401 harboring SCO3285 behind its own promoter	This work.
pGWS1110	pHJL401 harboring SCO3286 behind its own promoter	This work.
pGWS1111	pIJ2587 with SCO2259 promoter region (−587/+707 relative to the start of SCO2259)	This work.
pGWS1112	pIJ2587 with SCO2260 promoter region (−566/+658 relative to the start of SCO2260)	This work.
pGWS1113	pIJ2587 with SCO3285 promoter region (−300/+212 relative to the start of SCO3285)	This work.
pGWS1114	pIJ2587 with SCO3286 promoter region (−300/+763 relative to the start of SCO3286)	This work.

Heat and SDS sensitivity tests

To determine heat resistance of spores, spore suspensions were diluted to 10^4 spores/mL in 20% glycerol and incubated at 60 ºC for 5, 10 and 20 minutes. To test SDS sensitivity, SDS (5% w/v end concentration) or water (control) was added to spore suspensions and incubated at room temperature for 1 hr. After heat or SDS treatment, the suspensions were diluted and plated on SFM agar, followed by incubation for 2 days at 30 ºC. Survival rate was calculated as the ratio of colony forming units (cfu) with and without heat or SDS treatment.

Microscopy

Electron microscopy

For morphological studies of surface-grown aerial hyphae and spores of *S. coelicolor* M145 and its mutant derivatives by cryo-scanning electron (cryo-SEM), specimens were quickly frozen in liquid nitrogen slush and transferred directly to the cryo-transfer attachment of the microscope. Specimens were subsequently sputter-coated with a 2 nm layer of gold and examined using a JEOL JSM6700F scanning electron microscope.

Samples for the analysis of cross-sections of hyphae and spores via transmission electron microscopy (TEM) were prepared as follows. Slices of mycelium were cut from agar plates and placed in a fixative containing 1.5% (wt/vol) glutaraldehyde in 0.1 M cacodylate buffer (pH 7.4; 360 mosmol) at room temperature for 20 h. Post-fixation was performed in 1% (wt/vol) osmium tetroxide in phosphate buffer (pH 7.3; 330 mosmol) at room temperature for 2 h. After rinsing, samples were dehydrated in a graded series of ethanol, and then incubated in a graded series of epoxy resin LX-112 (Ladd Research Industries, Burlington, Vt.) in propylene oxide. The sample blocks were then placed in capsules filled with epoxy resin and polymerized at 60°C for 72 h. Ultrathin sections (70 nm) were cut on an ultramicrotome (Reichert OM U3), collected on copper grids, stained with uranyl acetate and lead hydroxide, and examined in a Philips EM410 transmission electron microscope.

Fluorescence microscopy

Fluorescence and corresponding light micrographs were obtained with a Zeiss Axioscope A1 upright fluorescence microscope (with an Axiocam Mrc5 camera at a resolution of 37.5 nm/pixel), with, for the green channel, 470- to 490-nm excitation and 515 long-pass detection; and for the red channel, 530- to 550-nm excitation and 590 long-pass detection. The green fluorescent images were created using 470/40-nm bandpass excitation and 525/50 bandpass detection; for the red channel, 550/25-nm bandpass excitation and 605/70 bandpass detection were used. For staining of the cell wall (peptidoglycan), we used TRITC-

WGA; for membrane staining, we used FM5-95 (both obtained from Molecular Probes). All images were background-corrected, setting the signal outside the hyphae to 0 to obtain a sufficiently dark background. These corrections were made using Adobe Photoshop CS5.

Computer analyses

DNA and protein databank searches were performed using the BLAST server of the National Center for Biotechnology Information at the National Institute of Health, Bethesda, MD, USA (http://www.ncbi.nlm.nih.gov) and the *S. coelicolor* genome page services (http://strepdb.streptomyces.org.uk/). Protein interactions were determined using the STRING database of known and predicted protein interactions (www.string-db.org).

Supplemental Material

Table S1. *Oligonucleotides used in this study.*

Name	5'-3' sequence	Purpose and restriction sites
2259_LF-1500	gtcagaattcggccgccgccctgctgccggacagc	Cloning, EcoRI
2259_LR+9	gtcagaagttatccatcacctctagagccggtcacgggggttttgtcc	Cloning, XbaI
2259_RF-9	gtcagaagttatcgcgcatctctagactcgtctgacgcctgccacacg	Cloning, XbaI
2259_RR+1500	gtcaaagcttcgccgacgagctgctggagcggttc	Cloning, HindIII
2260_LF-1169	gtcagaattctcagcggcggatgccgtgtcgt	Cloning, EcoRI
2260_LR+9	gtcagaagttatccatcacctctagaggtggacatggaactccctg	Cloning, XbaI
2260_RF-9	gtcagaagttatcgcgcatctctagaggcggatgaggccgctcagc	Cloning, XbaI
2260_RR+1500	gtcaaagcttgccagcaccgtcgcacccgcccgg	Cloning, HindIII
3285_LF-1500	gtcagaattcagcacgtgcgcaccaatgaggcgc	Cloning, EcoRI
3285_LR+9	gtcagaagttatccatcacctctagaggtggccatgagcggttcg	Cloning, XbaI
3285_RF-9	gtcagaagttatcgcgcatctctagagagcggtgagcgcggggccg	Cloning, XbaI
3285_RR+1500	gtcaaagcttggcgacagccgtccgctccccttcc	Cloning, HindIII
3286_LF-1500	gtcagaattctaggaggggccacgacccggtag	Cloning, EcoRI
3286_LR+9	gtcagaagttatccatcacctctagagacttccatggcatacgtcc	Cloning, XbaI
3286_RF-9	gtcagaagttatcgcgcatctctagaagggtctgaccggccatcacc	Cloning, XbaI
3286_RR+1500	gtcaaagcttcaggaggcggcgagcgcccggtag	Cloning, HindIII
2259_IFD_fw_+263	tgctcggcgaagccggtccaggt	PCR confirmation
2259_IFD_rev_-260	tcctggtgctgatgccgttgcag	PCR confirmation
2260_IFD_fw_+653	agggcttcgaagtgccgggtctc	PCR confirmation
2260_IFD_rev_-646	ccggcaagctcgtcgtcgactgc	PCR confirmation
3285_IFD_fw_+240	acgtgcagaacctgacggtctcg	PCR confirmation
3285_IFD_rev_-470	agcacgtcgcggactggacgctg	PCR confirmation
3286_IFD_fw_+541	tgcatcgaccgatccgaccagtg	PCR confirmation
3286_IFD_rev_-500	agcggtgcaggtccgcgaactcc	PCR confirmation
p2259_fw_eco_new	gtcagaattcgccgtgcacacgacggcgaacag	2259 own promoter, EcoRI
SCO2259SacI-rev	cacggtaccggcgcggttgagctccccggc	2259 pt 1 rv, KpnI, SacI
2259_pt.2_fw_Eco	gtcagaattctccacgcggagctgctcagc	2259 pt 2 fw, EcoRI
SCO2259MluI-rev	gccggtaccctgccacgcgtccagctcc	2259 pt 2 rv, KpnI, MluI
SCO2259MluI-fw	cgctctagagctggacgcgtggcagaaccc	2259 pt 3 fw, XbaI, MluI
2259_comp_rv_Hind_Bam	gtcaaagcttggatcctcagacgagggcgacggcctcc	2259 pt 3 rv (+Stop), HindIII, BamHI
2259_rev_XbaHind	aagctttctagagacgagggcgacggcctcctgc	2259 pt 3 rv GFP fusion, HindIII, XbaI
p2260_fw_eco_new	gtcagaattcagcgcgtcgtcgagcacgac	2260 own promoter, EcoRI
2260_comp_rv_Hind_Bam	gtcaaagcttggatcctcatccgcccggcgtgcacagc	2260 rv (+Stop), HindIII, BamHI
2260_rev_XbaHind_new	gtcaaagctttctagatccgcccggcgtgcacagcgg	2260 rv GFP fusion, HindIII, XbaI
3285_comp_fw_EcoRI	gtcagaattcacggctcgtcgagcttcaccgacg	3285 own promoter, EcoRI

3285_p1rv_BglII	aagcttagcgcgtcgtagatctcggtcc	3285 pt 1 rv, HindIII, BglII
3285_pt2fw_BglII	gaattccggaccgagatctacgacgcgct	3285 pt 2 fw, EcoRI, BglII
3285_p2_rev_PstI	aagcttgaactcgtcgaggcgcagctgcag	3285 pt 2 rv, HindIII, PstI
3285_p3_fw_PstI	gaattcatcaccggaggccggctgcagct	3285 pt 3 fw, EcoRI, PstI
3285_comp_rv_Hind_Bam	gtcaaagcttggatcctcaccgctccgttccgccggcc	3285 pt 3 rv (+Stop), HindIII, BamHI
3285_p3_rev_XbaHind	aagctttctagaccgctccgttccgccggccgcgt	3285 pt 3 rv GFP fusion, HindIII, XbaI
3286_comp_fw_EcoRI	gtcagaattccggacgatgacgacgaagacgacg	3286 own promoter, EcoRI
3286_comp_rv_Hind_Bam	gtcaaagcttggatcctcagaccctggccgtgccgttcagg	3286 rv (+Stop), HindIII, BamHI
3286_rev_XbaHind	gtcaaagctttctagagaccctggccgtgccgttcagg	3286 rv GFP fusion, HindIII, XbaI